PAPER

Optical nonlinearities in non-peripherally substituted pyridyloxy phthalocyanines: a combined effect of symmetry, ring-strain and demetallation

Kayode Sanusi, Edith Antunes and Tebello Nyokong*

The optical nonlinearities of six non-peripherally-substituted pyridyloxy phthalocyanines have been studied at 532 nm using a nanosecond Z-scan technique in a dimethyl sulphoxide solution. Ring-strain effects and the absence of a metal center were found to greatly reduce the inherent high nonlinearities expected of some of these phthalocyanine complexes. Of the six molecules investigated, 1(4), 8(11),15(18),22(25)-tetrakis-(2-pyridyloxy)phthalocyaninato lead(II) **3**, 1(4),8(11),15(18),22(25)-tetrakis-(2-pyridyloxy)phthalocyanine **5**, and 1(4),8(11),15(18),22(25)-tetrakis-(4-pyridyloxy)phthalocyanine **6** were found to exhibit negligible nonlinear optical behavior, due to either the absence of asymmetry or central metal and/or the presence of a ring-strain effect. A two-photon absorption process was found to be the major contributor to the observed reverse saturable absorption (RSA) in 1(4),8(11),15(18), 22(25)-tetrakis-(4-pyridyloxy)phthalocyaninato lead(II) **4**, 1(4)-mono-(2-pyridyloxy)phthalocyaninato lead(II) **7**, and 1(4)-mono-(4-pyridyloxy)phthalocyaninato lead(II) **8**, with large two-photon absorption cross-section, high hyperpolarizability and high third-order susceptibility values in the range of 4.53×10^{-43}–5.33×10^{-42} cm^4 s per photon, 1.61×10^{-28}–1.89×10^{-27} esu and 9.73×10^{-12}–7.05×10^{-11} esu respectively.

Introduction

Nonlinear optical (NLO) materials play a major role in the technologies that require light harvesting, storage, control and transmission. Examples of such areas of applications include photonics, optoelectronics and optical limiting.[1–4] Among the organic molecules that possess good NLO properties are the metallophthalocyanines (MPcs).[5–8] Their potential applications as optical limiters, optical switches and optical signal-processing devices have been extensively investigated.[9–14] The large optical nonlinearities of phthalocyanines (Pcs) are due to the presence of delocalized π electrons which confer on them some dipole moments that are fundamentally responsible for their NLO behaviors.[15–17]

A significant number of symmetrical Pcs, both metallated and unmetallated, have been extensively investigated for NLO applications.[5,8,18–21] Many of the studied Pcs show good NLO properties by reverse saturable absorption (RSA) through multi-photon absorption (nPA) mechanisms.[19,20] Low symmetry Pcs show improved NLO properties compared to their symmetrical analogues as a result of the increased molecular dipole moments.[22,23]

Trends in the third order nonlinear susceptibility $\chi^{(3)}$ in Pc isomers, which are crucial in understanding the relationship between the molecular electronic properties and the optical limiting (OL) responses in Pcs, have received little or no attention. The dependence of $\chi^{(3)}$ on the molecular architecture of a variety of organic molecules has been previously reported.[24,25] Non-peripherally substituted Pcs were employed in this work because of their lower aggregation tendencies and highly red-shifted linear absorption bands (Q-bands), compared to their peripherally substituted analogues.[26–28] The red shifting is important since it may result in the reduction of interferences resulting from the linear absorption of the materials in the measured nonlinear absorption (NLA) properties. NLA resulting from two photon absorption (2PA) dependent RSA is believed to take place in the region where the molecules have no linear absorption at all.[29]

In this paper, we present our findings on the NLA behavior of 1(4),8(11),15(18),22(25)-tetrakis-(2-pyridyloxy)phthalocyaninato lead(II) (**3**), 1(4),8(11),15(18),22(25)-tetrakis-(4-pyridyloxy)-phthalocyaninato lead(II) (**4**), 1(4)-mono-(2-pyridyloxy)phthalocyaninato lead(II) (**7**) and 1(4)-mono-(4-pyridyloxy)phthalocyaninato lead(II) (**8**) (Schemes 1 and 2). Molecules with similar substituents to those investigated here are known;[30–33] however, those containing lead have not been previously reported. Lead phthalocyanines (PbPcs) are known to possess good OL properties owing to the heavy atom effect[5,27,34] and

Department of Chemistry, Rhodes University, Grahamstown 6140, South Africa.
E-mail: t.nyokong@ru.ac.za
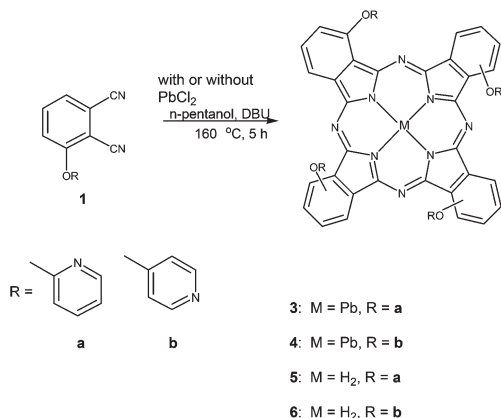
Scheme 1 Synthesis of tetrapyridyloxy Pcs **3–6**. For **3** and **4**, PbCl$_2$ was employed and left out for **5** and **6**.
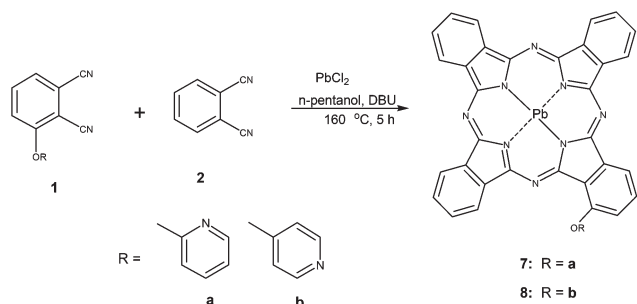
Scheme 2 Synthesis of monopyridyloxy PbPc complexes **7** and **8**.

the structural deformation caused by the metal being out of the plane of the ring in a "shuttle-cock" arrangement.[34,35] These observations suggested the use of metal-free analogues as an approach to determining the contributions of the central lead metal in the OL performances of PbPcs.

The metal-free Pcs analogous to complexes **3** and **4**, 1(4),8(11),15(18),22(25)-tetrakis-(2-pyridyloxy)phthalocyanine (**5**) and 1(4),8(11),15(18),22(25)-tetrakis-(4-pyridyloxy)phthalocyanine (**6**) (Scheme 1) were prepared and investigated.

Experimental

Materials

Dichloromethane (DCM), 1,8-diazabicyclo[5.4.0]undec-7-ene (DBU), *n*-pentanol, diethylether, ethanol, acetone, lead(II) chloride and 1,2-dicyanobenzene were obtained from Sigma Aldrich. Deuterated dimethyl sulphoxide (DMSO-d_6), *n*-hexane, methanol, dimethyl formamide (DMF) and dimethyl sulphoxide (DMSO) were purchased from Merck. All solvents were of reagent grade and were freshly distilled before use. 3-(Pyridin-2-yloxy)phthalonitrile (**1a**) and 3-(pyridin-4-yloxy)phthalonitrile (**1b**) were synthesized according to the reported procedure.[30–33]

Equipment and methods

Infra-red spectra were collected on a Perkin-Elmer Universal ATR Sampling accessory spectrum 100 FT-IR spectrometer. [1]H

NMR spectra were obtained using a Bruker AVANCE 600 MHz NMR spectrometer in DMSO-d_6. Elemental analyses were done using a Vario-Elementar Microcube ELIII, while mass spectra data were collected on a Bruker AutoFLEX III Smart-beam TOF/TOF mass spectrometer using α-cyano-4-hydrocinnamic acid as the matrix in the positive ion mode.

All *Z*-scan experiments described in this study were performed using a frequency-doubled Nd:YAG laser (Quanta-Ray, 1.5 J/10 ns fwhm pulse duration) as the excitation source. The laser was operated in a near Gaussian transverse mode at 532 nm (second harmonic), with a pulse repetition rate of 10 Hz and an energy range of 0.1 μJ–0.1 mJ, limited by the energy detectors (Coherent J5-09). The low repetition rate of the laser prevents cumulative thermal nonlinearities. The beam was spatially filtered to remove the higher order modes and tightly focused with a 15 cm focal length lens. The *Z*-scan system size ($l \times w \times h$) used was 600 mm × 300 mm × 350 mm (excluding the computer, energy meter, translation stage driver and laser system). The liquid samples were placed in a cuvette (internal dimensions: 2 mm × 10 mm × 55 mm, 0.7 mL) and a path length of 2 mm (Starna 21-G-2).

The nanosecond absorption spectroscopy set-up to investigate the triplet state behaviors was comprised of coupled laser systems, a Nd-YAG laser (already described above) pumping Lambda-Physik FL3002 dye (Pyridin 1 dye in methanol) laser. The analyzing beam source was a Thermo Oriel 66902 xenon arc lamp. A Kratos Lis Projekte MLIS-X3 photomultiplier coupled with a monochromator allows for selective excitation at wavelengths between 400 and 850 nm when required. Signals recorded with a two-channel, 300 MHz digital real time oscilloscope (Tektronix TDS 3032C).

Ground state electronic absorption spectra were recorded on a Shimadzu UV-2550 spectrophotometer. Fluorescence emission spectra were recorded on a Varian Eclipse spectro-fluorimeter. Fluorescence decay times were measured using a time correlated single photon counting (TCSPC) setup (Fluo-Time 200, Picoquant GmbH). The excitation source was a diode laser (LDH-P-670 driven by PDL 800-B, 670 nm, 20 MHz repetition rate, 44 ps pulse width, Picoquant GmbH). The details of the set-up have been previously described.[36]

Thermo-gravimetric analysis (TGA) was performed using a Perkin Elmer TGA 7 analyzer. The analyses were carried out under nitrogen at a flow rate of 120 cm^3 min^{-1}. The weighed sample masses were heated from 50 to 650 °C at a heating rate of 10 °C min^{-1}.

Synthesis

1(4),8(11),15(18),22(25)-Tetrakis-(2-pyridyloxy)phthalocyaninato lead(II) (3) (Scheme 1). A mixture of 3-(pyridin-2-yloxy)phthalo-nitrile (**1a**) (0.50 g, 2.26 mmol), *n*-pentanol (7.5 mL) and 0.25 mL of DBU was stirred under reflux at 160 °C for 5 h. The reaction was carried out under argon in the presence of an excess of metal salt, lead(II) chloride (0.33 g, 1.19 mmol). The crude product was cooled to room temperature and washed respectively in methanol, ethanol, *n*-hexane and diethylether by centrifugation and was allowed to dry in air. Further

purification of the compound was achieved by Soxhlet extraction using diethylether, water and *n*-hexane as solvents in succession. Column chromatography with silica gel as a stationary phase and DCM–DMF (3 : 1) as an eluent was also performed. The product was thereafter concentrated, dried and ground, before a final washing in *n*-hexane to afford the pure compound.

Complex **3** yield: (65%). UV-Vis (DMSO): λ_{max}/nm, (log ε): 711 (5.10), 639 (3.68), 365–463 (3.63), 366 (4.25). FT-IR [KBr disc (ν_{max}/cm^{-1})]: 3066 (C–H aromatic), 1655 (C=N imine), 1572, 1532, 1465, 1427 (C=C aromatic), 1289, 1242, 1139, 1089, 1011 (C–O–C), 894, 869, 826, 657 (Pc-Skeleton). ^{1}H NMR (600 MHz, DMSO-d_6): δ, ppm: 8.76–8.89 (4*H*, m, pyridyloxy-*H*), 8.58–8.60 (4*H*, d, pyridyloxyl-*H*), 8.39–8.41 (2*H*, m, Pc-*H*), 8.20–8.28 (2*H*, d, Pc-*H*), 8.00–8.16 (2*H*, m, Pc-*H*), 7.92–7.96 (2*H*, d, Pc-*H*), 7.79–7.85 (2*H*, d, Pc-*H*), 7.71–7.72 (2*H*, d, Pc-*H*), 7.68–7.69 (4*H*, d, pyridyloxy-*H*), 7.12–7.19 (4*H*, m, pyridyloxy-*H*). Anal. Calc. for $C_{52}H_{28}N_{12}O_4Pb$ (hexane): C 59.08, H 3.57, N 14.26; found: C 59.23, H 3.63, N 13.76. MS (MALDI-TOF) *m/z*: calcd 1092; found: 1096 $[M + 4H]^+$.

1(4),8(11),15(18),22(25)-Tetrakis-(4-pyridyloxy)phthalocyaninato lead(ɪɪ) (4) (Scheme 1). The synthesis and purification of **4** was as outlined for **3** except that 3-(pyridin-4-yloxy)phthalonitrile (**1b**) was employed instead of 3-(pyridin-2-yloxy)phthalonitrile (**1a**). However, only the Soxhlet procedure was employed to afford the pure compound.

Complex **4** yield: (75%). UV-Vis (DMSO): λ_{max}/nm, (log ε): 716 (5.20), 645 (3.68), 355–459 (3.58), 356 (4.05). FT-IR [KBr disc (ν_{max}/cm^{-1})]: 3288 (C–H aromatic), 1634 (C=N imine), 1480, 1405 (C=C aromatic), 1329, 1261, 1192, 1112, 1087, 1024, 1001 (C–O–C), 959, 870, 842, 811, 745 (Pc-Skeleton). ^{1}H NMR (600 MHz, DMSO-d_6): δ, ppm: 6.79–6.83 (8*H*, d, pyridyloxy-*H*), 6.62–6.64 (2*H*, d, Pc-*H*), 7.09–7.16 (2*H*, d, Pc-*H*), 7.30–7.36 (2*H*, m, Pc-*H*), 6.37–6.40 (2*H*, d, Pc-*H*), 7.54–7.56 (2*H*, m, Pc-*H*), 7.60–7.63 (2*H*, d, Pc-*H*), 8.14–8.17 (8*H*, d, pyridyloxy-*H*). Anal. Calc. for $C_{52}H_{28}N_{12}O_4Pb$ (hexane): C 59.08, H 3.57, N 14.26; found: C 58.70, H 4.16, N 13.67. MS (MALDI-TOF) *m/z*: calcd 1092; found: 1094 $[M + 2H]^+$.

1(4),8(11),15(18),22(25)-Tetrakis-(2-pyridyloxy) (5) and 1(4), 8(11),15(18),22(25)-tetrakis-(4-pyridyloxy) (6) phthalocyanines (Scheme 1). The synthesis and purification of **5** and **6** were similar except that 3-(pyridin-2-yloxy)phthalonitrile (**1a**) (0.30 g, 0.34 mmol) was employed for **5** and 3-(pyridin-4-yloxy)-phthalonitrile (**1b**) (0.30 g, 0.34 mmol) for **6**. The phthalonitriles respectively were refluxed under argon at 160 °C for 5 h in the presence of DBU (0.25 mL) as a catalyst and *n*-pentanol (5 mL) as the solvent. The crude products were washed several times in *n*-hexane and diethylether before the final purification on a silica gel column. The stationary phase was packed using an ethanol–DCM (4 : 1) solvent system; however, the compounds were eluted using DMF as the solvent. The DMF fraction was concentrated, dried, ground and washed several times with warm water before recrystallizing from acetone.

Complex **5** yield: (72%). UV-Vis (DMSO): λ_{max}/nm, (log ε): 681 (4.32), 617 (3.75), 390–424 (3.96), 351 (4.16). FT-IR [KBr disc (ν_{max}/cm^{-1})]: 3052 (C–H aromatic), 1656 (C=N, imine),

1572, 1532, 1480, 1428 (C=C aromatic), 1368, 1337, 1290, 1259, 1248, 1147, 1075, 1054 (C–O–C), 893, 841, 814, 764, 743, 729, 682 (Pc-Skeleton). ^{1}H NMR (600 MHz, DMSO-d_6): δ, ppm: 7.91–7.94 (4*H*, m, pyridyloxy-*H*), 6.31–6.34 (4*H*, m, pyridyloxy-*H*), 7.78–7.79 (4*H*, d, pyridyloxy-*H*), 6.48–6.50 (4*H*, d, pyridyl-oxy-*H*), 7.0–7.1 (2*H*, d, Pc-*H*), 7.53–7.56 (2*H*, m, Pc-*H*), 7.67–7.68 (2*H*, d, Pc-*H*), 7.14–7.18 (2*H*, m, Pc-*H*), 7.21–7.22 (2*H*, d, Pc-*H*), 6.94–6.96 (2*H*, d, Pc-*H*). Anal. Calc. for $C_{52}H_{30}N_{12}O_4 \cdot 7H_2O$: C 61.60, H 4.34, N 16.57; found: C 61.31, H 4.20, N 15.58.

MS (MALDI-TOF) *m/z*: calcd 887; found: 889 $[M + 2H]^+$.

Complex **6** yield: (70%). UV-Vis (DMSO): λ_{max}/nm, (log ε): 685 (4.69), 617 (3.75), 376–409 (3.99), 330 (4.16). FT-IR [KBr disc (ν_{max}/cm^{-1})]: 3067 (C–H aromatic), 1632 (C=N, imine), 1548, 1480, 1402 (C=C aromatic), 1331, 1271, 1190, 1117, 1086, 1043 (C–O–C), 967, 887, 846, 810, 744 (Pc-Skeleton). ^{1}H NMR (600 MHz, DMSO-d_6): δ, ppm: 6.90–6.91 (2*H*, d, Pc-*H*), 6.18–6.30 (2*H*, d, Pc-*H*), 7.44–7.59 (8*H*, d, pyridyloxy-*H*), 7.66–7.86 (2*H*, m, Pc-*H*), 7.90–7.95 (2*H*, d, Pc-*H*), 8.71–8.72 (8*H*, d, pyridyloxy-*H*), 8.00–8.20 (2*H*, d, Pc-*H*), 8.44–8.49 (2*H*, m, Pc-*H*). Anal. Calc. for $C_{52}H_{30}N_{12}O_4 \cdot 6H_2O$: C 62.71, H 4.22, N 16.88; found: C 62.56, H 4.21, N 16.01. MS (MALDI-TOF) *m/z*: calcd 887; found: 889 $[M + 2H]^+$.

1(4)-Mono-(2-pyridyloxy)phthalocyaninato lead(ɪɪ) (7) (Scheme 2). A mixture of 3-(pyridin-2-yloxy)phthalonitrile (**1a**) (0.25 g, 1.13 mmol) and 1,2-dicyanobenzene (**2**) (0.75 g, 5.86 mmol) was firstly homogenized and subsequently placed in a round bottom flask containing *n*-pentanol (10 mL) and lead(ɪɪ) chloride (2.0 g, 7.19 mmol). The mixture was then refluxed at 160 °C for 5 h in the presence of DBU (0.25 mL) as a catalyst, with continuous stirring under an inert atmosphere. The mixture thereafter was cooled to room temperature, and washed successively in methanol, ethanol, *n*-hexane and diethylether. The product was further purified using a Soxhlet apparatus with *n*-hexane, water, diethylether and acetone as solvents respectively. Only acetone dissolved one of the components of the products. The acetone fraction was then concentrated, re-purified again in a Soxhlet apparatus with *n*-hexane as a solvent and analyzed. The result was found to correspond to the desired compound.

Complex **7** yield: (15%). UV-Vis (DMSO): λ_{max}/nm, (log ε): 704 (4.87), 635 (3.67), 404–463 (3.60), 331 (4.12). FT-IR [KBr disc (ν_{max}/cm^{-1})]: 3154 (C–H aromatic), 1658 (C=N imine), 1571, 1532, 1482, 1429 (C=C aromatic), 1362, 1292, 1186, 1048, 1011 (C–O–C), 890, 872, 764, 739, 716, 687 (Pc-Skeleton). ^{1}H NMR (600 MHz, DMSO-d_6): δ, ppm: 8.06–8.15 (2*H*, d, Pc-*H*), 9.41–9.52 (2*H*, m, Pc-*H*), 8.58–8.60 (2*H*, d, Pc-*H*), 8.31–8.50 (4*H*, m, Pc-*H*), 9.00–9.03 (1*H*, d, Pc-*H*), 9.27–9.29 (2*H*, d, Pc-*H*), 8.20–8.25 (1*H*, m, Pc-*H*), 7.33–7.36 (1*H*, d, Pc-*H*), 7.83–7.92 (2*H*, d, pyridyloxy-*H*), 9.52–9.54 (2*H*, d, pyridyloxy-*H*). Anal. Calc. for $C_{37}H_{19}N_9OPb$ (hexane): C 57.40, H 3.67, N 14.02; found: C 57.32, H 3.19, N 14.25. MS (MALDI-TOF) *m/z*: calcd 813; found: 816 $[M + 3H]^+$.

1(4)-Mono-(4-pyridyloxy)phthalocyaninato lead(ɪɪ) (8) (Scheme 2). The synthesis and purification of **8** were as outlined for **7** but 3-(pyridin-4-yloxy)phthalonitrile (**1b**) was

employed instead of 3-(pyridin-2-yloxy)phthalonitrile (**1a**). Here also, the acetone extract from the Soxhlet was concentrated, dried and re-purified again in a Soxhlet apparatus with *n*-hexane as a solvent.

Complex **8** yield: (17%). UV-Vis (DMSO): λ_{max}/nm, (log ε): 705 (5.08), 635 (3.70), 402–462 (3.58), 334 (4.11). FT-IR [KBr disc (ν_{max}/cm^{-1})]: 3180 (C–H aromatic), 1637 (C=N, imine), 1574, 1522, 1478, (C=C aromatic), 1394, 1361, 1329, 1259, 1159, 1074, 1011 (C–O–C), 881, 795, 771, 741, 720 (Pc-Skeleton). ^{1}H NMR (600 MHz, DMSO-d_6): δ, ppm: 6.96–6.99 (1H, d, Pc-H), 7.05–7.07 (1H, d, Pc-H), 7.10–7.16 (1H, m, Pc-H), 7.01–7.04 (2H, d, pridyloxy-H), 9.01–9.04 (2H, d, pyridyloxy-H), 7.76–7.83 (6H, m, Pc-H), 7.90–7.91 (3H, d, Pc-H), 8.14–8.17 (3H, d, Pc-H). Anal. Calc. for $C_{37}H_{19}N_9OPb$ (hexane): C 57.40, H 3.67, N 14.02; found: C 57.85, H 3.42, N 14.05. MS (MALDI-TOF) *m/z*: calcd 813; found: 813 [M]$^+$.

Photophysical parameters

Fluorescence (Φ_F) and triplet (Φ_T) quantum yields were determined in DMSO by the comparative methods described before[37–40] using ZnPc in DMSO as a standard. $\Phi_F = 0.2$[38] and $\Phi_T = 0.65$[40] for ZnPc as a standard in DMSO.

Z-Scan measurements

The *Z*-scan experiment was performed according to the method described by Sheik-Bahae *et al.*[41–43] Assuming a Gaussian spatial and temporal pulse, and using the open aperture (OA) *Z*-Scan theory for multi-photon absorption (*n*PA) by Sutherland,[44] the general equation for OA normalized transmittance can be written as eqn (1)[19]

$$T_{OA(2PA)} = \frac{1}{1 + \beta_2 L_{eff}(I_{00}/(1 + (z/z_0)^2))} \qquad (1)$$

where I_{00} is the on-focus intensity (peak input intensity), β_2 is the two photon absorption coefficient, L_{eff}, z and z_0 are the effective path length in the sample of length L, translation distance of the sample relative to the focus and Rayleigh length, respectively. The Rayleigh length is defined as $\pi w_o^2/\lambda$, where λ is the wavelength of the laser and w_o is the beam waist at the focus ($z = 0$). L_{eff} is given by eqn (2):

$$L_{eff} = \frac{1 - e^{-\alpha L}}{\alpha} \qquad (2)$$

where α is the linear absorption coefficient.

Eqn (1) is an analytical expression for OA transmittance for two-photon absorbers, where other terms such as three photon absorption are ignored. The good agreement between the experimental and theoretical 2PA transmittances was further substantiated by plotting $1/T$ (1/transmittance) *versus* I_0 (incident intensity), eqn (3), which is a standard expression for a pure 2PA process in wavelength regions where there is no linear absorption.[29,45]

$$1/T = 1 + \beta_2 g^{(2)} I_0 L \qquad (3)$$

where β_2 is the 2PA coefficient as defined above, $g^{(2)}$ is the degree of second-order coherence of the laser pulses, I_0 is the incident intensity, L is the sample path length and T is the transmittance. The linearity of this plot confirmed the findings from the previous analysis (eqn (1)) that the observed RSA was largely due to 2PA. The β_2 values are those obtained from the fittings with eqn (1).

The molecular two-photon absorption (2PA) cross-section σ_2 (in units of cm^4 s per photon) is calculated from the 2PA coefficient using eqn (4):[29]

$$\sigma_2 = \frac{1000 \, h\nu\beta_2}{N_A C} \qquad (4)$$

where N_A is the Avogadro constant, C is the sample concentration, and $h\nu$ is the photon energy of an incident photon in joules.

The imaginary component of the third order susceptibility ($I_m [\chi^{(3)}]$) is given by eqn (5):[46]

$$I_m [\chi^{(3)}] = n^2 \varepsilon_0 c\lambda\beta_2 / 2\pi \qquad (5)$$

where n and c are the linear refractive index and the speed of light respectively, ε_0 is the permittivity of free space, and λ and β_2 terms are as described above.

Second order hyperpolarizability (γ) of the material was determined using eqn (6):[47]

$$\gamma = \frac{I_m[\chi^{(3)}]}{f^4 C_{mol} N_A} \qquad (6)$$

where N_A is the Avogadro constant as defined above, C_{mol} is the concentration of the active species in the triplet state per mole and f is the Lorentz local field factor given as $f = (n^2 + 2)/3$.

Results and discussion

Characterization of Pc complexes

Schemes 1 and 2 show the synthetic routes for the preparation of compounds **3–8**. The synthesis of **7** and **8** as examples of low symmetry metallophthalocyanine (MPc) complexes involved a statistical mixed condensation method.[48] This method involves two different phthalonitrile precursors in a 1 : 3 mole ratio (Scheme 2). The method usually results in the formation of a mixture of products, and to obtain the target compound requires systematic separation and extensive purification techniques.

The structural analyses of all the new complexes were satisfactory and consistent with the predicted structures as shown in Schemes 1 and 2. The complexes were successfully characterized with spectroscopic techniques such as the UV-Vis, MALDI-TOF MS, IR, ^{1}H NMR and elemental analyses. Apart from the disappearance of the nitrile vibrational band at the 2220–2250 cm^{-1} region in the phthalonitriles on forming the Pcs, the intensity of bands in the finger-print region also increased upon cyclization, serving as evidence for the

formation of highly aromatic compounds. The ^{1}H NMR spectra showed clearly the isomeric difference between the compounds with respect to the position of the pyridyl nitrogen atom(s). The inner NH protons in the Pc cavity were not observed for the metal-free Pcs; however, the UV-vis and the other spectroscopic data corroborate the proposed structures. The C, H and N elemental analysis data of the complexes are consistent with solvated Pcs, with the PbPcs found to contain 1 molecule of hexane each, while compounds **5** and **6** contained 7 and 6 molecules of water respectively. This is in agreement with observations in the chemical literature that Pcs are often isolated as solvates.[31,48–50]

The thermal properties of these compounds were investigated by thermogravimetric analysis (TGA). An initial decomposition step occurred between 50 and 150 °C, particularly for **6** and to a lesser extent for **3**, suggesting loss of any incorporated solvents (as evidenced from the elemental analysis data). The main decomposition step for the phthalocyanines was observed to take place above 250 °C for complex **3** and, more clearly, for complex **6**, while the monosubstituted Pc (**7**) exhibited a slow decomposition step, indicating good thermal stability, over the temperature range studied, Fig. 1. Pcs and their related compounds are generally known to decompose at temperatures above 250 °C.[50–52] For compound **7**, an increase in %weight was observed immediately below 100 °C, and we assumed this to be due to the adsorption of N_2 gas onto the sample's surface in the heating chamber, with the presumption that it occurred because the thermal-stability analysis was done under an N_2 atmosphere.

The ground state electronic spectra and properties of compounds **3–8** are presented (Fig. 2 and Table 1). The absorption spectra for the non-peripherally substituted lead phthalocyanine (PbPc) complexes (**3**, **4**, **7** and **8**) in DMSO showed monomeric behavior, evidenced by single and narrow Q-bands, and typical of non-aggregated metallo-phthalocyanines (MPcs).[53] The split Q-bands were not observed for the metal-free Pcs (**5** and **6**) because of the basic nature of the solvent (DMSO) used,[53] and this may also be responsible for the non-observance of the NH proton resonance peak in the NMR, since the solvent was also DMSO. The red shifting of the Q band of **4** relative to **3** is evidence of the proposed ring-strain
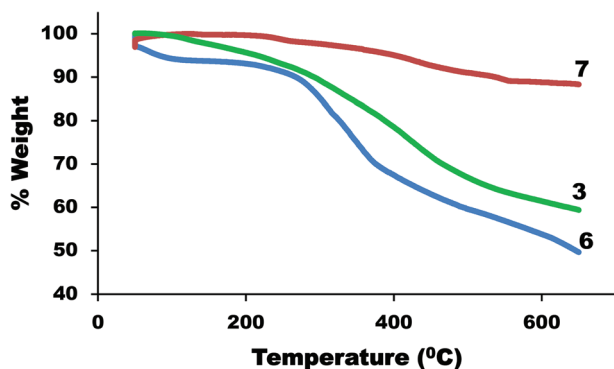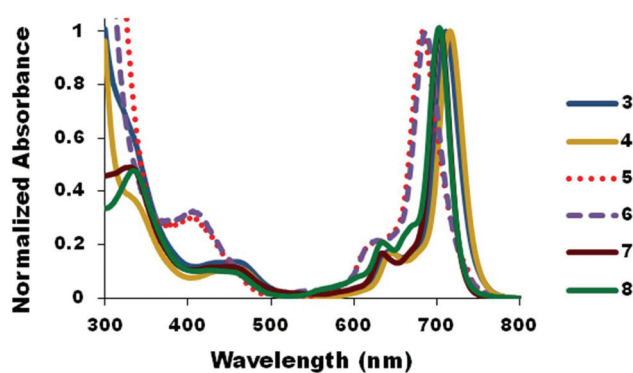

Fig. 2 Ground state electronic absorption spectra of 1(4),8(11),15(18),22 (25)-tetrakis-(2-pyridyloxy)phthalocyaninato lead(ⅱ) (**3**), 1(4),8(11),15 (18),22(25)- tetrakis-(4-pyridyloxy)phthalocyaninato lead(ⅱ) (**4**), 1(4),8 (11),15(18),22(25)- tetrakis-(2-pyridyloxy)phthalocyanine (**5**), 1(4),8 (11),15(18),22(25)-tetrakis-(4-pyridyloxy)phthalocyanine (**6**), 1(4)-mono- (2-pyridyloxy)phthalocyaninato lead(ⅱ) (**7**) and 1(4)-mono-(4-pyridyloxy) phthalocyaninato lead(ⅱ) **8**, in DMSO. Concentration ≈1.0 × 10^{-5} M.

effect in **3**, to be discussed below (Fig. 3). This effect strongly attenuates the degree of electron polarization in the molecules during light perturbation, hence allowing them to absorb in the higher energy part of the electromagnetic spectrum. A similar trend was observed in the metal-free derivatives, **5** and **6**. Also, the Q-bands of the tetra-pyridyloxy **3** and **4**, are more red-shifted compared to the mono-pyridyloxy derivatives, **7** and **8** respectively, due to the presence of a higher number of pyridyl-oxy substituents in the former. Nitrogen containing Pcs show red shifted Q bands.[54]

Also of interest in the UV-Vis absorption spectra are the observed bands at 365–463, 355–459, 390–424, 376–409, 404–463 and 402–462 nm for compounds **3**, **4**, **5**, **6**, **7** and **8** respectively. A detailed explanation of the genesis of similar bands at around 485 nm in tetra(α-amino) zinc phthalocyanine, $ZnPc(\alpha\text{-}NH_2)_4$,[55] and between 400 and 500 nm in MPcs with axial amino ligands has been documented.[56,57] These bands were convincingly ascribed to the effect of charge transfer (CT) transitions from the ligands (amino substituents) to the aromatic phthalocyanine ring. Similarly for these compounds (**3**, **4**, **5**, **6**, **7** and **8**), we may assign these bands to CT from the pyridyl groups to the phthalocyanine ring of the complexes, where the CT is even expected to be more prominent because of the inclusive position of the pyridyl nitrogen atoms in the aromatic Pc ring.

Photophysical properties

The fluorescence quantum yields (Φ_F) presented in Table 1 revealed the poor luminescent behavior of the lead Pcs, owing to the heavy atom effect which is expected to promote intersystem crossing to the triplet states.[5,34] Thus, the measured values were generally <0.1 for all the studied lead Pcs. In addition to the heavy atom effect, n → π* transitions resulting from the pyridyl electrons also contributed to the fluorescence inhibition.[55,58] Similar to the PbPcs, a low Φ_F value of 0.02 was measured for compound **6**, due to the n → π*

Fig. 1 TGA profiles for compound **3**, **6** and **7**.

Table 1 Electronic and photophysical properties of the studied complexes in DMSO at room temperature

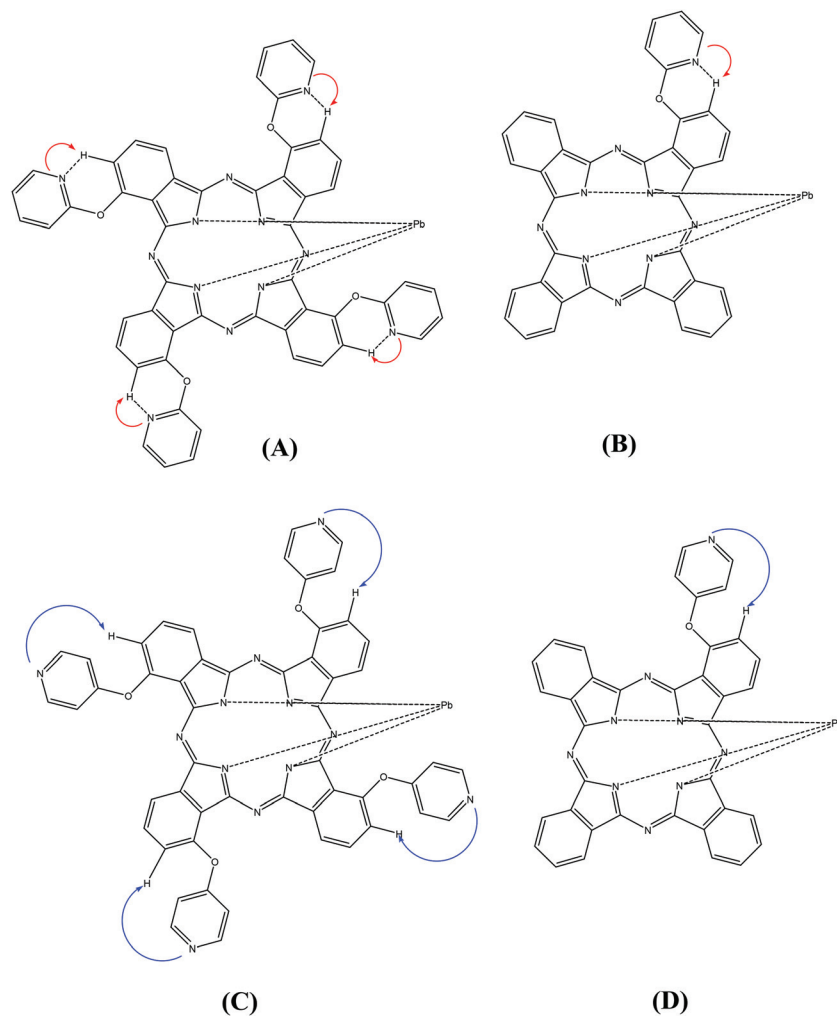| Complex	Q-band (nm)	$\lambda_{em,max}$ (nm)	$\lambda_{exc,max}$ (nm)	Φ_F	Φ_T	τ_T (µs)	τ_F (ns)
3	711	691	678	0.08	—	—	4.85 ± 0.01 (66.9%)
							2.62 ± 0.01 (33.1%)
4	716	696	686	0.03	—	—	4.19 ± 0.01 (95.4%)
							0.87 ± 0.06 (4.6%)
5	683	694	683	0.11	0.25	205.0 ± 8.1	4.96 ± 0.01 (100%)
6	686	701	688	0.02	0.10	76.0 ± 3.8	4.06 ± 0.01 (100%)
7	704	691	684	<0.01	—	—	3.06 ± 0.01 (94.5%)
							0.13 ± 0.01 (5.5%)
8	705	696	689	0.02	—	—	3.21 ± 0.01 (96.0%)
							0.45 ± 0.04 (4.0%)

Fig. 3 Proposed excited-state structures for **3**, **4**, **7** and **8**. All four bonds that connect the central lead metal to the Pc ring are dashed bonds, and are meant to depict demetallation upon excitation. Ring-strain effects as a result of the close proximities between the lone pair of electrons on the pyridyl nitrogen atoms and the β-H atoms of compounds **3** (A) and **7** (B) are shown by red arrows, while the wide gaps between these similar atoms in **4** (C) and **8** (D) are shown by blue arrows (the wide gaps prevent ring-strain).

transitions which resulted in intersystem crossing (ISC) into the triplet states.[55,58] This was however not observed in compound **5**, and may be explained based on the ring-strain effect, which engaged its non-bonding electrons on excitation, thus encouraging fluorescence and resulting in a higher Φ_F value of 0.11, Table 1. The ring-strain effect arose from the electrostatic interaction between the β-H atom of the Pc ring and the lone pair of electron(s) on the pyridyl nitrogen atom(s) on exposure to light, as shown in Fig. 3A and 3B for the metallated derivatives.

The attempt to compare the measured Φ_F values with the triplet quantum yield values Φ_T, especially in the PbPcs, was not successful; this could be as a result of the short triplet lifetimes due to the heavy atom effects.[5,34,59] The non-observance of any triplet state transition for the PbPcs may also depend on the pulse duration (10 ns) and the pulse repetition rate (10 Hz) of the laser system employed.[60] However for the metal-free Pcs, the time-resolved triplet absorption and singlet depletion decays were observed as expected for an unmetallated Pc molecule. The Φ_T values obtained for these metal-free isomers, 0.25 and 0.10, for **5** and **6** respectively (Table 1), did suggest that the molecules behaved differently from the electronic singlet states in the triplet states. One would have expected compound **6** with a lower Φ_F value to have the higher Φ_T value since fluorescence and ISC to the triplet states are competing processes. The triplet lifetimes τ_T measured for these molecules, 205.0 and 76.0 μs for **5** and **6** respectively (Table 1), deviate from the expected, since it is expected that molecules with large triplet quantum yields will have correspondingly shorter lifetimes,[59] but this is not the case for **5** and **6**. And since the molecules essentially have the same molecular weight, it may be appropriate to say that their different excited state properties are due to their different structural configurations in these various excited states.

All the lead pyridyloxy Pcs gave blue-shifted emission spectra relative to the absorption spectra (Fig. 4A and B), a phenomenon that has been reported before for PbPc complexes and was attributed to the loss of the central lead metal upon excitation.[28,61] The single absorption and the split excitation spectra, of compound **8** in toluene, again proved the demetallation assertion upon excitation, Fig. 5. The demetallation of PbPcs is common on excitation because of the "shuttlecock" configuration.[28,34,35,61] Complexes **5** and **6** show the expected fluorescence behavior, with excitation spectra similar to the absorption spectra, and both are mirror images of the emission spectra, Fig. 4C.

Time correlated single photon counting (TCSPC) experiments gave two fluorescence lifetimes (τ_F) for each of the PbPc complexes **3**, **4**, **7** and **8** (Table 1), hence suggesting the existence of two different compositions for each molecule in the excited singlet state. Since the PbPc complexes demetallate on excitation, it is possible that the two lifetimes are due to metallated and demetallated species. The longer lifetime may be attributed to the demetallated Pc while the shorter lifetime is due to the metallated Pc. It is known that H_2Pcs (and Pcs containing smaller central metals) exhibit longer fluorescence lifetimes compared to MPcs containing larger central metals.[62] The longer τ_F of the two lifetimes has the higher percentage of abundance confirming the domination of demetallation. The demetallated form of each of the Pcs may be associated with the longer τ_F as well as the higher abundance. However for the metal-free Pcs, **5** and **6** (Table 1), single lifetimes (τ_F) were observed, thus confirming the purity of the compounds. The measured lifetimes also followed the expected trend with compound **5** having higher τ_F as compared to **6**.
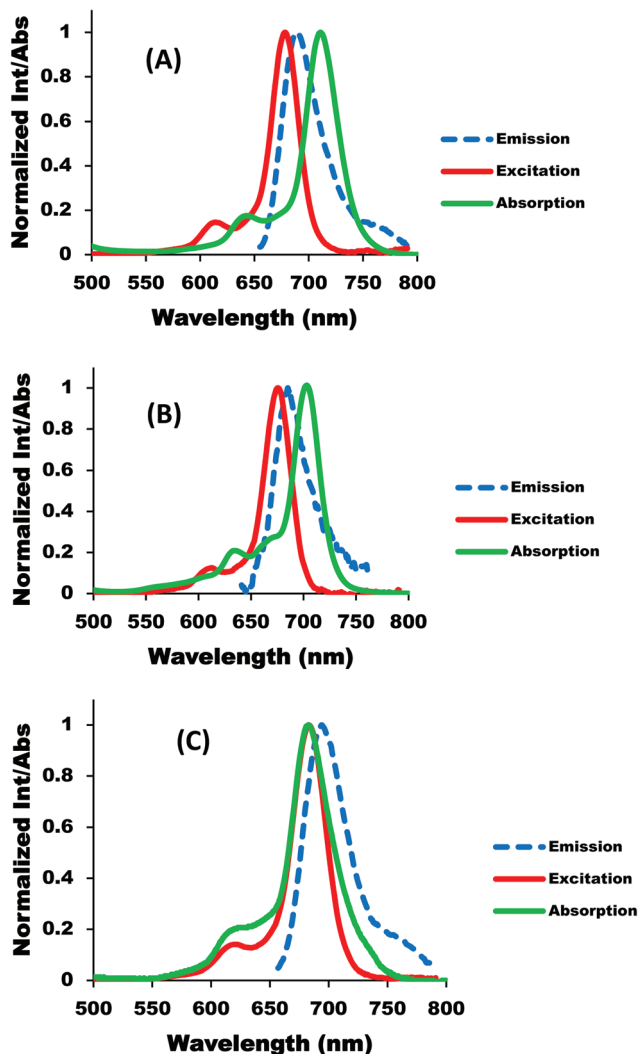

Fig. 4 Absorption, emission and excitation spectra of complexes **3** (A), **8** (B) and **5** (C) in DMSO; concentration ≈1.0 × 10⁻⁶ M.
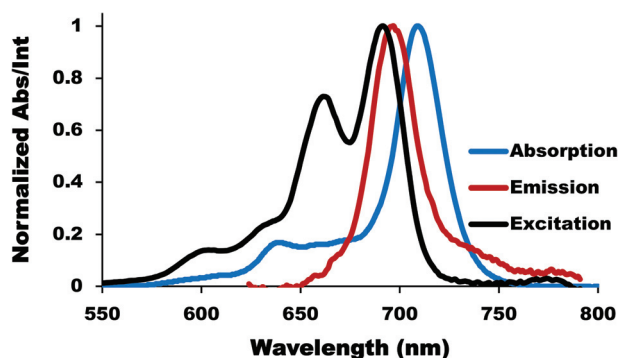

Fig. 5 Absorption, emission and excitation spectra of compound **8** in toluene; concentration ≈1.0 × 10⁻⁶ M.

Nonlinear optical (NLO) parameters

Nonlinear absorption (NLA) behavior. Fig. 6 shows the representative OA Z-scans for the studied Pcs (**3–8**) at 2.8 A and
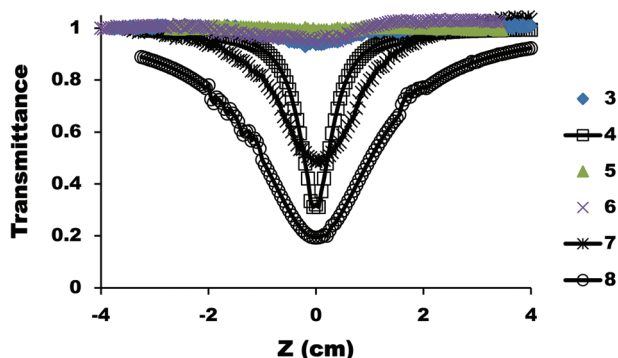
Fig. 6 Open aperture Z-scan signatures of the studied complexes (3–8). $I_{00} \approx 150$ MW cm^{-2}, abs. = 2.8 in DMSO.

ca. 150 MW cm^{-2} on-axis peak input intensity. We observed strong NLA behaviors in compounds **4**, **7** and **8**, with their profiles being of the reverse saturable absorption (RSA) kind.[16,19,21,22,34,41–44] The values of the minimum transmittance in these compounds (**4**, **7** and **8**) dropped below 50% of the linear transmission (Fig. 6), which makes them good candidates for optical limiting applications.[4,6,19,22] The Z-scan data for compounds **3**, **5** and **6** showed negligible RSA, which cannot sufficiently cause any significant optical limiting effect in the samples (Fig. 6). A similar behavior was observed under the different experimental conditions employed such as the different peak input intensities and absorbances. This behavior was, however, not expected, especially for compound **3** which is a PbPc, since PbPcs are known to show good NLO behaviour.[5,27,34] The negligible RSA observed in complex **3** could be due to the ring strain effect discussed above. The ring-strain effect was reduced in compound **7** compared to **3**, since only one of these interactions is available in the molecule's structure (Fig. 3B). Complexes **5** and **6** have no heavy atom effect; hence they show negligible RSA.

We assume that the demetallation of the central Pb metal initiates the 2PA, which has been identified as the underlining mechanism for the observed RSA in these molecules (**4**, **7** and **8**). It thus appears that the absence of a ring-strain effect (Fig. 3C and 3D), and the presence of a central lead metal, would entrust good optical limiting properties on pyridyloxy Pcs as observed for compounds **4** and **8**.

The analyses of the Z-scan results for **4**, **7** and **8** as mentioned above were done by fitting the data to a 2PA function from which we obtained the 2PA coefficients (β_2). Further analysis to obtain the NLO parameters for compounds **3**, **5** and **6** was not necessary because of their poor NLA responses. The measured 2PA coefficients for **4**, **7** and **8** under different experimental conditions are presented in Fig. 7. The values were found to vary with sample concentration (absorbance) and the on-axis input peak intensities (I_{00}). A plot of β_2 *versus* I_{00} showed an exponential decrease of β_2 as I_{00} increases, Fig. 7 A. It was believed that for multi-photon absorption (*n*PA) dependent RSA, the values of β_n should be invariant with changes in the on-axis peak irradiance, I_{00}.[19,59,63] An
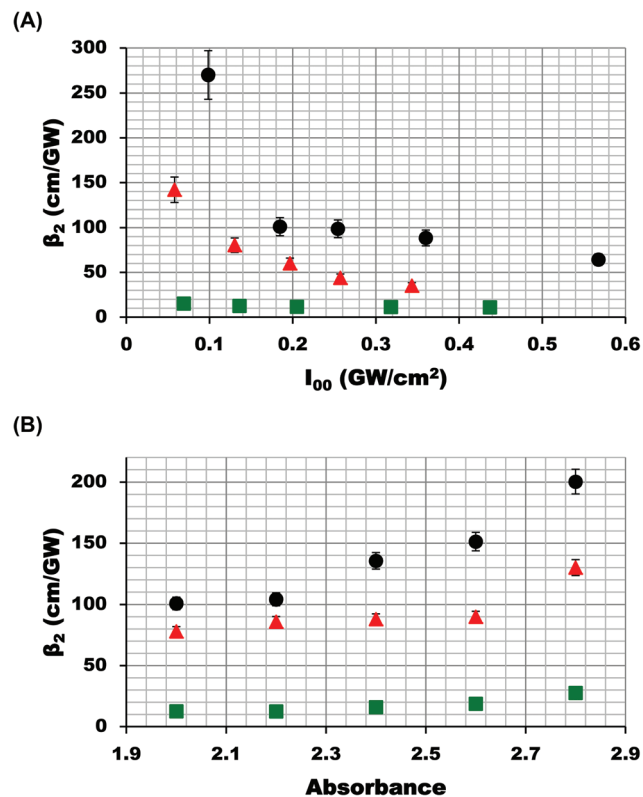

Fig. 7 Plots showing (A) the peak intensity (I_{00}) dependence on β_2 and (B) the concentration (absorbance) dependence on β_2 for compounds **4** (▲), **7** (■), and **8** (●). Each data point for each sample represents an independent Z-scan measurement. Abs. = 2.0 for each sample in (A). $I_{00} \approx 150$ MW cm^{-2} for each independent measurement in (B).

exponential decrease in β_n as I_{00} increases has also been reported in the literature.[6,64–66] We believe that the observed RSA was due to 2PA, and the decrease in β_2 as I_{00} increases is a consequence of the depletion of the two-photon absorbing species in the S_0 state (Fig. 7A), which has been termed here as the *ground singlet state depletion*.

A plot of β_2 *versus* the sample concentration (absorbance) showed an exponential increase in β_2 with increasing absorbance values, Fig. 7B. This observation suggests that the β_2 depends strongly on the number of statistically available two-photon absorbers in the excited state, thus resulting in an increase in the 2PA cross-sections (σ_2) as S_0 is de-populated (Fig. 7B). It is worth noting that the measured 2PA cross-sections reported here ($\sigma_2 = 4.56 \times 10^{-42}$ and 5.33×10^{-42} cm^4 s per photon for **4** and **8** respectively, Table 2) are among the highest reported so far in the literature for nonlinear optical materials with pulsed laser illumination.[29,65,67]

To further ascertain the underlining mechanism for the observed RSA, we analyzed the Z-scan results by performing a plot of the transmittance (*T*) *versus* the input fluence (I_0), Fig. 8. The plots showed an exponential decrease in transmittance with increasing input irradiance. A similar observation has been reported before for organic molecules doped in solid materials, and it was ascribed to 2PA.[67] This observation may

Table 2 Nonlinear optical properties of samples **4**, **7** and **8** in DMSO at 2.8 A. All data were obtained with 10 ns pulses at 532 nm wavelength. The peak intensity for each measurement was ≈150 MW cm^{-2}

Complex	β_2 (cm GW^{-1})	I_m [$\chi^{(3)}$] (esu)	γ (esu)	σ_2 (cm^4 s per photon)	I_{lim} (J cm^{-2})
4	130.00	4.58×10^{-11}	1.62×10^{-27}	4.56×10^{-42}	0.55
7	27.63	9.73×10^{-12}	1.61×10^{-28}	4.53×10^{-43}	0.80
8	200.30	7.05×10^{-11}	1.89×10^{-27}	5.33×10^{-42}	0.32
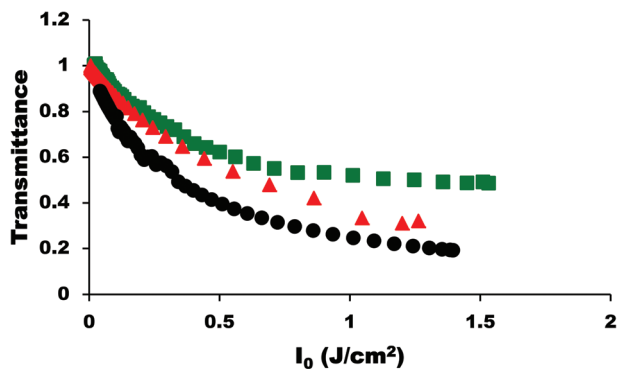
Fig. 8 Transmittance *versus* input fluence (I_0) curves for compounds **4** (▲), **7** (■) and **8** (●) at 2.8 abs. and *ca.* 150 MW cm^{-2} peak input intensity (I_{00}) for each sample.

Fig. 9 Intensity-dependent transmission of compounds **4** (▲), **7** (■) and **8** (●) at absorption of 2.8. $I_{00} \approx 150$ MW cm^{-2} for each measurement.

Table 3 The relationship between the samples' absorbance and the probability factor, $g^{(2)}$

Complex	Abs.	$g^{(2)}$ (%)
4	2.0	8.0
	2.4	7.5
	2.8	5.8
7	2.0	26
	2.4	23
	2.8	18
8	2.0	8.0
	2.4	9.0
	2.8	7.0

be assumed to result from the increasing population of the two-photon absorbers in the triplet state T$_1$ (where the NLA occurs) as the beam intensity increases, hence causing a continuous decrease in the transmittance, *T*. The region at infinite irradiances where the transmittance (*T*) no longer varies with further increase in the input fluence may be termed as the *saturation points.* The lowest input fluence at which this starts to occur may be described as the *saturation fluence.*[60] The saturation points may be defined as the points where further increase in the beam irradiance no longer increases the statistical number of the available two-photon absorbers in the triplet state.

Analysis of the degree to which processes other than the speculated 2PA have contributed to the observed RSA was done by fitting the *Z*-scan data to the standard expression (eqn (3)) for a pure two-photon absorption process, Fig. 9. The parameter $g^{(2)}$ which may be interpreted as the degree to which other processes apart from the deduced 2PA have contributed to the observed NLO behavior is presented in Table 3, for three absorbances. We observed the lowest contributions from the other NLA processes for the most concentrated solution (absorbance = 2.8) for the three samples, Table 3. This suggests that the statistically available number of two-photon absorbers in the sample does influence the extent of contribution to the observed RSA by other NLA processes.

We propose a three-level model to describe the 2PA-induced RSA in these compounds (**4**, **7** and **8**), Fig. 10. The molecule in the S$_0$ state, after absorbing the first photon P1, undergoes a transition to the intermediate electronic state ('virtual') and
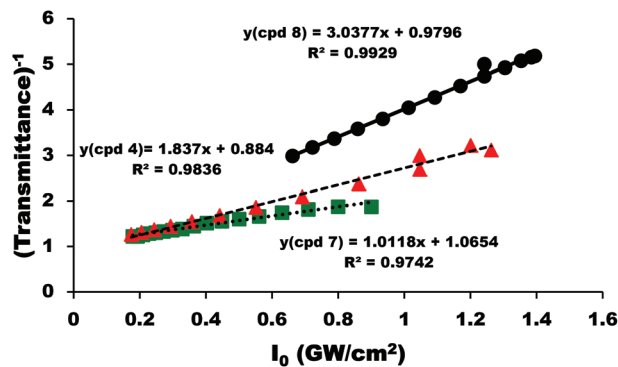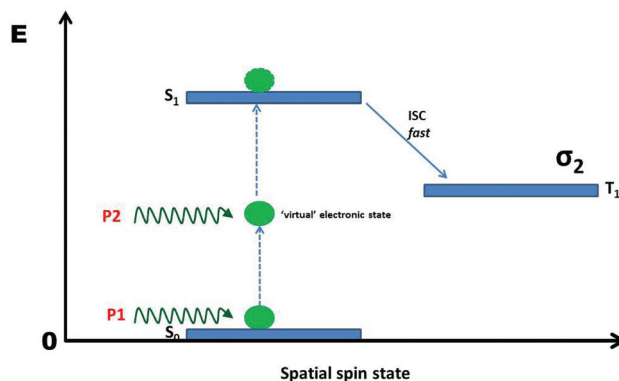

Fig. 10 Three-level model for the pyridyloxy Pcs (**4**, **7** and **8**).

becomes demetallated, from where it absorbs the second photon P2 to the real eigenstate S$_1$. The demetallation results from the structural instability induced by the heavy size of the central Pb atom, coupled with the intense effect of the incident photon energy. This thus describes a sequential 2PA for these systems. We assume that the molecules undergo a fast ISC rate to populate the triplet state T$_1$, where the NLA occurs.

Third-order nonlinear susceptibility and hyperpolarizability. The estimated hyperpolarizability γ values for the samples are given in Table 2. In general, the values of γ obtained under different experimental conditions (such as the absorbances and the on-axis input peak intensities) vary as expected in the

same trend as the measured 2PA coefficients (β_2). The physical interpretation of γ may be explained on the basis of the light–matter interaction. γ is induced when the interaction of light with the permanent dipole (μ) of a molecule causes a bias in the average orientation of the molecule. The value of γ depends on the energy difference of the charge transfer between the ground and the excited state, the energy of the incident photon, the difference in the dipole moment of the ground and excited states, and the transition dipole moment between the ground and excited states.[15] The larger the value of γ, the better the molecule as a nonlinear optical material. It is enhanced whenever the fundamental frequency and/or the doubled frequency are close to the charge transfer absorption band,[15,17] which is true in our case. Organo–metallic molecules with strong absorption bands in the UV-vis spectrum resulting from metal-to-ligand (MLCT) or ligand-to-metal (LMCT) electronic charge transfer transitions have been reported to possess large γ values,[15,17] which may explain the reason for our high γ values compared to those reported in the literature.[68,69] In addition, the absence of symmetry induces a dipole moment within the molecule. The larger the dipole moment within a molecule, the larger the γ value as observed for the low symmetry compound **8**, when compared to its tetra-substituted derivative **4**.

The imaginary component of the third-order nonlinear susceptibility $I_m[\chi^{(3)}]$ values calculated for the molecules is presented in Table 2. These values are required to be sufficiently large as they determine the fastness of an optical material in responding to the perturbation initiated by the intense laser beam. The values obtained in this study are found to be larger than those reported in the literature for organic molecules and Pcs embedded in polymer thin-films;[6,22,65,66,70] we therefore expect a superior NLO response with our Pcs in a solid state form, since these would make them more photo-chemically stable than in solution.[19,22,70]

Optical limiting. An important term in the optical limiting measurement is the limiting threshold (I_{lim}), defined as the input fluence at which the transmittance is 50% of the linear transmittance.[21] The lower the I_{lim} value, the better the material as an optical limiter. The optical limiting curves obtained for five of the compounds (**3**, **4**, **6**, **7** and **8**) are presented in Fig. 11. The Z-scan data for compound **5** could not be fitted; hence, we could not determine its associated w_o. This is not surprising because compound **5** suffers from both the absence of a central Pb metal and the presence of ring-strain effects. The poor NLA property of **3** and **6** can be clearly seen in Fig. 11, where their output fluence increases with the input fluence, thus giving similar profiles as the linear transmission (T), which is a case devoid of nonlinear absorption. For compounds **4**, **7** and **8**, however, good optical limiting effects were exhibited (Fig. 11), with I_{lim} of *ca* 0.55 J cm^{-2}, 0.80 J cm^{-2} and 0.32 J cm^{-2} for the compounds respectively, at 2.8 absorbance in DMSO. The value reported for Zn tetra *tert*-butyl phthalocyanine in chloroform, ~0.45 J cm^{-2},[19] is lower than what we obtained for compounds **4** and **7** respectively, but higher than that of compound **8**. We believe the optical
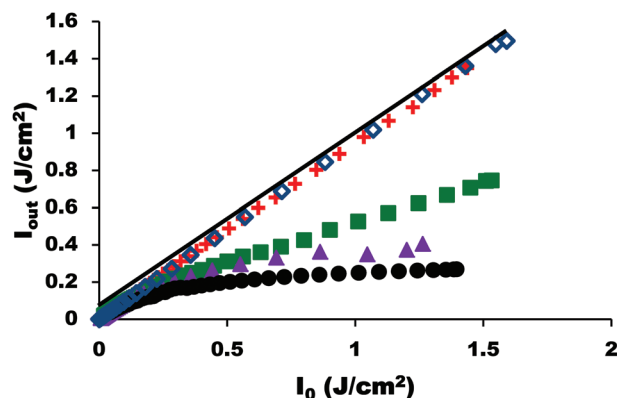

Fig. 11 Output fluence (I_{out}) *versus* input fluence (I_0) for compounds **3** (+), **4** (▲), **6** (□), **7** (■) and **8** (●) at 2.8 absorbance. The black solid line represents a case of linear transmission. Peak intensity (I_{00}) ≈ 150 MW cm^{-2} for each sample.

limiting performance of these compounds can be improved by increasing the concentration of the Pcs and also by incorporating them into a polymer matrix which will improve their photochemical stability.[6,19,22,66,70]

Conclusions

The processes involved in the NLA behaviors of six non-peripherally substituted pyridyloxy Pc complexes have been determined. The various factors that have contributed to the observed nonlinearities in the compounds have been fully described using the measured experimental data. Ring-strain effects were found to greatly reduce the nonlinearities inherent in the 2-pyridyloxy isomers (**3** and **5**), with the exception of the low symmetry derivative (compound **7**), which exhibits a considerable optical limiting property. We also observed demetallation in the PbPc derivatives, which brings about 2PA upon excitation. The synergistic effect of the absence of demetallation and the presence of ring-strain was responsible for the poor NLA behavior observed in compound **5**, while for compound **6**, the poor NLA was due primarily to the absence of a central Pb metal that could bring about the demetallation. The nonlinear absorptions observed in **4**, **7** and **8** have thus been attributed to 2PA. The measured 2PA cross-section, second-order hyperpolarizability and third-order susceptibility values were found to be comparatively large, making the compounds important materials for consideration in many photonics and optoelectronics fields.

Acknowledgements

Notes and references

1 R. W. Boyd, in *Nonlinear Optics*, Academic Press, San Diego, CA, 1992.

2 J. Zyss, in *Molecular Nonlinear Optics: Materials, Physics and Devices*, Academic Press, New York, 1994.

3 B. E. A. Saleh and M. C. Teich, in *Fundamentals of Photonics*, Wiley, New York, 1991.

4 L. De Boni, S. D. Corrêa and C. R. Mendonça, in *Advances in Lasers and Electro Optics*, ed. N. Costa and A. Cartaxo, INTECH, Croatia, 2010, p. 838, ISBN 978-953-307-088-9, downloaded from SCIYO.COM.

5 J. S. Shirk, R. G. S. Pong, F. J. Bartoli and A. W. Snow, *J. Appl. Phys. Lett.*, 1993, **63**, 1880.

6 P. K. Hegde, A. V. Adhikari, M. G. Manjunatha, P. Poornesh and G. Umesh, *Opt. Mater.*, 2009, **31**, 1000.

7 F. E. Hernandez, S. Yang, E. W. Van Stryland and D. Hagan, *J. Opt. Lett.*, 2000, **25**, 1180.

8 J. W. Perry, K. Mansour, I. Y. S. Lee, X. L. Wu, P. V. Bedworth, C. T. Chen, D. Ng, S. R. Marder, P. Miles, T. Wada, M. Tian and H. Sasabe, *Science*, 1996, **273**, 1533.

9 G. de la Torre, P. Vazquez, F. Agullo-Lopez and T. Torres, *Chem. Rev.*, 2004, **104**, 3723.

10 J. W. Perry, in *Nonlinear Optics of Organic Molecules and Polymers*, ed. H. S. Nalwa and S. Miyata, CRC Press, Boca Raton, FL, 1997, p. 813.

11 G. de la Torre, P. Vazquez, F. Agullo-Lopez and T. Torres, *J. Mater. Chem.*, 1998, **8**, 1671.

12 G. de la Torre, T. Torres and F. Agullo-Lopez, *Adv. Mater.*, 1997, **9**, 265.

13 H. S. Nalwa and J. S. Shirk, in *Phthalocyanines. Properties and Applications*, ed. C. C. Leznoff and A. B. P. Lever, VCH Publishers (LSK) Ltd, Cambridge, U.K., 1996, vol. 4, p. 79.

14 S. R. Flom, in *Porphyrin and Phthalocyanine Handbook*, ed. K. M. Kadish and K. M. Smith and R. Guilard, Academic Press, Boston, MA, 2003.

15 T. Verbiest, S. Houbrechts, M. Kauranen, K. Clays and A. Persoons, *J. Mater. Chem.*, 1997, **7**, 2175.

16 A. Major, F. Yoshino, J. S. Aitchison and P. W. E. Smith, *Proc. SPIE*, 2005, **5724**, 269.

17 A. M. McDonagh, M. G. Humphrey, M. Samoc and B. Luther-Davies, *Organometallics*, 1999, **18**, 5195.

18 Y. Chen, W. Y. Duoyuan and L. Y. Nie, *J. Opt. Mater.*, 2003, **24**, 581.

19 R. S. S. Kumar, S. V. Rao, L. Giribabu and D. N. Rao, *Chem. Phys. Lett.*, 2007, **447**, 274.

20 S. Hughes, G. Spruce, B. S. Wherrett and T. Kobayashi, *J. Appl. Phys.*, 1997, **81**, 5905.

21 Y. Chen, L. Gao, M. Feng, L. Gu, N. He, J. Wang, Y. Araki, W. J. Blau and O. Ito, *Mini-Rev. Org. Chem.*, 2009, **6**, 55.

22 S. J. Mathews, S. C. Kumar, L. Giribabu and S. V. Rao, *Opt. Commun.*, 2007, **280**, 206.

23 S. V. Rao, P. T. Anusha, T. S. Prashant, D. Swain and S. P. Tewari, *Mater. Sci. Appl.*, 2011, **2**, 299.

24 J. S. Shirk, J. R. Lindle, F. J. Bartolli and M. E. Boyle, *J. Phys. Chem.*, 1992, **96**, 5847.

25 J. S. Shirk, J. R. Lindle, F. J. Bartolli, Z. H. Kafafi, A. W. Snow and M. E. Boyle, *Int. J. Nonlinear Opt. Phys.*, 1992, **1**, 699.

26 J. Mark and M. J. Stillman, *J. Am. Chem. Soc.*, 1994, **116**, 1292.

27 M. Konami, M. Hatano and A. Tajiri, *Chem. Phys. Lett.*, 1990, **166**, 605.

28 D. K. Modibane and T. Nyokong, *Polyhedron*, 2008, **27**, 1102.

29 J. E. Ehrlich, X. L. Wu, I.-Y. S. Lee, Z.-Y. Hu, H. Röckel, S. R. Marde and J. W. Perry, *J. Opt. Lett.*, 1997, **22**, 1843.

30 W. Chidawanyika, A. Ogunsipe and T. Nyokong, *New J. Chem.*, 2007, **31**, 377.

31 N. Masilela and T. Nyokong, *Dyes Pigm.*, 2010, **84**, 242.

32 W. Chidawanyika and T. Nyokong, *J. Photochem. Photobiol., A*, 2009, **202**, 99.

33 S. Gaspard and T. H. Tran-Thi, *J. Chem. Soc., Perkin Trans. 2*, 1989, 383.

34 J. W. Perry, K. Mansour, S. R. Marder, D. Alvarez Jr., K. J. Perry and I. Choong, *J. Opt. Lett.*, 1994, **19**, 625.

35 A. S. Nizovtsev and S. G. Kozlova, *J. Phys. Chem. A*, 2013, **117**, 481.

36 N. Masilela and T. Nyokong, *J. Photochem. Photobiol., A*, 2011, **223**, 124.

37 S. Fery-Forgues and D. Lavabre, *J. Chem. Educ.*, 1999, **76**, 1260.

38 A. Ogunsipe, J. Y. Chen and T. Nyokong, *New J. Chem.*, 2004, **7**, 822.

39 T. H. Tran-Thi, C. Desforge and C. Thiec, *J. Phys. Chem.*, 1989, **93**, 1226.

40 P. Kubat and J. Mosinger, *J. Photochem. Photobiol., A*, 1996, **96**, 93.

41 M. Sheik-Bahae, A. A. Said and E. W. Stryland, *Opt. Lett.*, 1989, **14**, 955.

42 M. Sheik-Bahae, A. A. Said, T. Wei, D. J. Hagan and E. W. Van Stryland, *IEEE J. Quantum Electron.*, 1990, **26**, 760.

43 E. W. Van Stryland and M. Sheik-Bahae, in *Characterization Techniques and Tabulations for Organic Nonlinear Materials*, ed. M. G. Kuzyk and C. W. Dirk, Marcel Dekker, Inc., 1998, pp. 655–692.

44 R. I. Sutherland, in *Handbook of Nonlinear Optics*, Marcel Dekker, New York, NY, 2nd edn, 2003, Revised and expanded.

45 R. Loudon, in *The Quantum Theory of Light*, Oxford U. Press, London, 1973.

46 E. M. García-Frutos, S. M. O'Flaherty, E. M. Maya, G. de la Torre, W. Blau, P. Vázqueza and T. Torres, *J. Mater. Chem.*, 2003, **13**, 749.

47 D. Dini and M. Hanack, in *The Porphyrin Handbook: Physical Properties of Phthalocyanine-based Materials*, ed. K. M. Kadish, K. M. Smith and R. Guilard, Academic Press, USA, 2003, vol. 17, pp. 22–31.

48 N. Masilela and T. Nyokong, *Synth. Met.*, 2012, **162**, 1839.

49 N. Masilela and T. Nyokong, *J. Lumin.*, 2010, **130**, 1787.

50 J. Rusanova, M. Pilkington and S. Decurtins, *Chem. Commun.*, 2002, 2236.

51 R. O. Ogbodu, E. Antunes and T. Nyokong, *Dalton Trans.*, 2013, **42**, 10769.

52 S. A. Znoiko, V. E. Maizlish, G. P. Shaposhnikov, N. Sh. Lebedeva and E. A. Mal'kova, *Russ. J. Phys. Chem. A*, 2013, **87**, 352.

53 M. J. Stillman and T. Nyokong, in *Phthalocyanines - Properties and Applications*, ed. A. B. P. Lever and C. C. Leznoff, VCH, New York, 1989, ch. 3, vol. 1.

54 T. Nyokong, in *Structure and Bonding: Functional Phthalocyanine Molecular Materials*, ed. J. Jiang, Series Ed. D. M. P. Mingos, Springer, 2010, vol. 135, pp. 45–87.

55 X.-F. Zhang, X. Li, L. Niu, L. Sun and L. Liu, *J. Fluoresc.*, 2009, **19**, 947.

56 G. V. Ouedraogo, C. More, Y. Richard and D. Benlian, *Inorg. Chem.*, 1981, **20**, 4387.

57 B. W. Dale, *Trans. Faraday Soc.*, 1969, **65**, 331.

58 http://www.monzir-pal.net/Lab Manuals/Practical Instrumental Analysis/Instrument Book/Instbook/Fluorescence.htm

59 J. R. Darwent, P. Douglas, A. Harriman, G. Porter and M.-C. Richoux, *Coord. Chem. Rev.*, 1982, **44**, 83.

60 L. W. Tutt and T. F. Boggess, *Prog. Quant. Electr.*, 1993, **17**, 299.

61 D. K. Modibane and T. Nyokong, *Polyhedron*, 2009, **28**, 1475.

62 K. Ishii and N. Kobayashi, in *The Porphyrin Handbook*, ed. K. M. Kadish, K. M. Smith and R. Guilard, Elsevier, 2003, ch. 1, vol. 16.

63 P. Poornesh, K. Ravi, G. Umesh, P. K. Hegde, M. G. Manjunatha, K. B. Manjunatha and A. V. Adhikari, *Opt. Commun.*, 2010, **283**, 1519.

64 S. Couris, E. Koudoumas, A. A. Ruth and S. Leach, *J. Phys. B: At., Mol. Opt. Phys.*, 1995, **28**, 4537.

65 C. V. Bindhu, S. S. Harilal, V. P. N. Nampoori and C. P. G. Vallabhan, *Appl. Phys. B: Lasers Opt.*, 2000, **70**, 429.

66 P. Poornesh, G. Umesh, P. K. Hegde, M. G. Manjunatha, K. B. Manjunatha and A. V. Adhikari, *J. Appl. Phys. B*, 2009, **97**, 117.

67 S. H. Guang, R. Gvishi, P. N. Prasad and B. A. Reinhardt, *Opt. Commun.*, 1995, **117**, 133.

68 J. Britton, M. Durmuş, S. Khene, V. Chauke and T. Nyokong, *J. Phorphy. Phthalocya.*, 2013, **17**, 1.

69 J. Britton, C. Litwinski, M. Durmuş, V. Chauke and T. Nyokong, *J. Phorphy. Phthalocya.*, 2011, **15**, 1239.

70 M. Yüksek, A. Elmali, M. Durmuş, H. Yaglioglu, H. Ünver and T. Nyokong, *J. Opt.*, 2010, **12**, 1.